Title	Rapid hydrolysis of phosphate monoesters by zirconium(IV) complexes in neutral solution
Author(s)	Erxleben, Andrea; Coleman, Fergal
Publication Date	2012
Publication Information	Coleman, F,Erxleben, A (2012) 'Rapid hydrolysis of phosphate monoesters by zirconium(IV) complexes in neutral solution'. Polyhedron, 48 :104-109.
Link to publisher's version	http://dx.doi.org/10.1016/j.poly.2012.09.015
Item record	http://hdl.handle.net/10379/3985
DOI	http://dx.doi.org/http://dx.doi.org/10.1016/j.poly.2012.09.015

Rapid Hydrolysis of Phosphate Monoesters by Zirconium(IV) Complexes in Neutral Solution

Fergal Coleman, Andrea Erxleben*

School of Chemistry, National University of Ireland, Galway, Ireland.

* To whom correspondence should be addressed.

Email: andrea.erxleben@nuigalway.ie. Phone: +353 91 492483. Fax: +353 91 495576

Abstract

Three zirconium(IV) complexes (**1** – **3**) with mono- and dinucleating tripodal ligands are reported that promote the hydrolysis of the phosphate monoesters *p*-nitrophenyl phosphate (NPP) and phenyl phosphate (PP) in neutral solution. At pH 7 up to 10^4 and 10^6-fold rate accelerations of the hydrolysis of NPP and PP are observed. A detailed kinetic study has been carried out for NPP. The complexes show Michaelis-Menten behaviour, k_{cat} and $1/K_m$ values at pH 7.0, 25 °C are 2.7 x 10^{-5} s^{-1} and 806 M^{-1} (**1**), 1.1 x 10^{-4} s^{-1} and 556 M^{-1} (**2**) and 1.1 x 10^{-4} s^{-1} and 565 M^{-1} (**3**). Entropies of activation of -92.0 J K^{-1} mol^{-1} (**1**), -75.6 J K^{-1} mol^{-1} (**2**) and -98.6 J K^{-1} mol^{-1} (**3**) are consistent with an associative mechanism.

Keywords: Zirconium; Catalysis; Phosphate ester hydrolysis

1. Introduction

With the half-life for the spontaneous hydrolysis of dibasic alkyl phosphates being in the order of 10^{12} years at ambient temperature [1], phosphate monoester hydrolysis is one of the most difficult reactions catalyzed by an enzyme. Over the years, much effort has been devoted to the development and study of metal complexes that mimic the structure and function of natural phosphatases [2,3]. However, in many of these studies phosphate diesters are used as model substrates, although mono- and diester cleavage can take place by different mechanisms [4]. Generally, the uncatalyzed hydrolysis of phosphate diesters proceeds *via* an associative mechanism, while phosphate monoesters hydrolyze by a dissociative mechanism in the absence of any catalyst. Because of this and because phosphate monoesters are the true substrates of phosphatases, it is important to study the hydrolysis of both substrates separately.

The hydrolytic activity of Zr^{4+} towards phosphate esters has first been described 70 years ago [5]. 60 years later two detailed kinetic studies on the reaction of $ZrCl_4$ with the phosphate diester bis(*p*-nitrophenyl) phosphate and with a DNA dinucleotide

have been published [6,7]. Due to its high positive charge, small ionic radius, hard Lewis acid character and high acidity of Zr-OH_2 (formation of Zr-OH nucleophile at low pH), Zr^{4+} is a highly efficient catalyst for phosphate ester cleavage. Up to 9 orders of magnitude rate accelerations have been reported for $ZrCl_4$-mediated phosphate diester hydrolysis [6,7]. However, the solution chemistry of $ZrCl_4$ is governed by the formation of ill-defined polynuclear hydroxo-bridged species. Precipitation of Zr^{4+} at pH > 5.5 prevents significant catalytic activity of zirconium salts in neutral solution. Kennedy *et al.* studied NPP hydrolysis in the presence of gelatinous zirconium(IV) hydroxide as heterogenous catalyst [8]. They observed a modest 30-fold rate acceleration over the uncatalyzed reaction at pH 7. A small number of ligands have been investigated with the aim to develop Zr complexes that are soluble and active catalysts at neutral pH [6,9-11]. The most promising results were obtained with tris(hydroxomethyl)aminomethane [6,9]. When coordinated to Zr, the reactivity of the metal is retained in weakly acidic solution. However, an excess of the ligand is required and the activity decreases significantly at higher pH values which has been attributed to aggregation [6]. Stulz and Leumann showed that Zr tetraporphyrinate can provide up to 9 orders of magnitude rate accelerations for the transesterification of 2-hydroxypropyl phenyl phosphate and methyl phenyl phosphate in benzene/methanol [11]. Likewise, the Zr complex [$Zr(acac)_2$(sae)] (acac = acetylacetonate; sae = salicylidineaminoethanol) reported by the same authors [10] was found to be a highly efficient catalyst for phosphate diester cleavage in non-aqueous solution. However, in the presence of water, the cleavage rate dropped significantly. Evidently, the synthesis of additional Zr complexes that are stable, soluble and active at pH values close to neutrality is a key factor in the development of suitable catalytic systems and still needs more effort.

Here we report a mononuclear and two dinuclear Zr complexes that promote the hydrolysis of the phosphate monoesters *p*-nitrophenyl phosphate (NPP) and phenyl phosphate (PP). Interestingly, the Zr complexes are more reactive towards PP than towards NPP and the Zr complex promoted hydrolysis of the phosphate monoester NPP is faster than that of the phosphate diester bis(*p*-nitrophenyl) phosphate. To the best of our knowledge no detailed kinetic study on the hydrolysis of a phosphate monoester by a Zr complex has been described so far.

2. Experimental

2.1. General

Imino diacetate, diethyl iminodiacetate, *p*-methoxyphenol, zirconyl chloride ($[Zr_4(OH)_8(H_2O)_{16}]Cl_8 \cdot 12H_2O$), sodium phenyl phosphate, bis(*p*-nitrophenyl) phosphate (BNPP), and *p*-nitrophenyl phosphate (NPP) were purchased from Aldrich and used as supplied. All of the other chemicals and solvents were of analytical or spectroscopic grade, purchased from commercial sources and used without further purification. Deuterated solvents were obtained from Apollo Scientific. L^1, L^2, and L^3 were prepared according to literature procedures [12,13].

^1H and ^{31}P NMR spectra were recorded on a Jeol ECX-400 spectrometer. The pD values of D_2O solutions were measured by use of a glass electrode and addition of a value of 0.4 to the pH meter reading [14,15]. The pD values were adjusted using concentrated DNO_3 and NaOD solutions.

UV/Vis measurements were carried out on a Varian Cary 50 scan spectrophotometer coupled to a Grant thermostated water circulation bath. Mass spectra were obtained on an electrospray mass spectrometer (Waters LCT Premiere XE**)** in negative mode.

2.2. Kinetic measurements

The hydrolysis rates of NPP and BNPP were measured by monitoring the increase in the visible absorbance at 400 nm due to the release of the *p*-nitrophenolate anion. Rate constants were obtained by the initial rate method (< 5 % conversion). Concentrations of *p*-nitrophenolate were calculated from the extinction coefficient (18,700 M^{-1} cm^{-1}). Concentrations were corrected for the degree of ionization of *p*-nitrophenol at the respective pH value using pK_a (*p*-nitrophenol) = 7.16 [16]. In a typical experiment 15 µL of a freshly prepared BNPP or NPP stock solution (10 mM in water) were added to a solution of the Zr complex (3 mL, 0.25 – 2 mM) at 25 °C.

The Zr complexes were generated *in situ* by mixing $[Zr_4(OH)_8(H_2O)_{16}]Cl_8 \cdot 12H_2O$ with L^1 in a 1:4 ratio and by mixing $[Zr_4(OH)_8(H_2O)_{16}]Cl_8 \cdot 12H_2O$ with L^2 or L^3 in a 1:2 ratio. The metal complex solutions were buffered with 50 mM HEPES in the pH range 6.0 to 8.5. The ionic strength was maintained at 0.1 M with NaCl. Kinetic runs were run in duplicate to give a reproducibility of ± 15 %.

2.3. Activation parameters

The enthalpy of activation, $\Delta H^{\ddagger}$, entropy of activation, $\Delta S^{\ddagger}$, and activation energy, E_a, were obtained by measuring the pseudo-first-order rate constants k_{obs} at 25, 35, 45, and 55 °C (pH 7.0, 50 mM HEPES, I = 0.1 M (NaCl)). The data were plotted as $\ln(k_{obs}/T)$ against 1/T and fitted to the Eyring equation $\ln(k_{obs}/T) = -(\Delta H^{\ddagger}/RT) + \ln(k/h) + \Delta S^{\ddagger}/R$ where k is the Boltzmann constant, h is the Planck constant and R is the molar gas constant. E_a was determined by plotting $\ln k_{obs}$ against 1/T and fitting the data to the Arrhenius equation $\ln k_{obs} = \ln A - E_a/RT$.

3. Results and Discussion

*3.1. Formation and solution behaviour of the $[ZrL^1(H_{(2)}O)_x]^{n+}$ **(1)***

The zirconium complex of the tripodal ligand L^1 shown in Chart 1 was prepared *in situ* by mixing water soluble zirconyl chloride, $[Zr_4(OH)_8(H_2O)_{16}]Cl_8 \cdot 12H_2O$, and L^1 in a 1:4 ratio. At 2 mM concentration, clear solutions were obtained between pH 6 and 12. The ^{1}H NMR spectra (Fig. 1) recorded immediately after mixing clearly indicate the coordination of Zr to the trianionic, tetradentate ligand. Significant shifts of the signals in the aromatic region corroborate binding to the deprotonated phenolate oxygen. The methylene groups that give singlets in the ^{1}H NMR spectrum of the free ligand appear as doublets of doublets due to chelate ring formation. At pH values < 6 an extremely fine white powder precipitated which was isolated by centrifugation. However, elemental analysis results varied from sample to sample. Energy dispersive X-ray spectroscopy showed a low consistency of Zr content within

samples which suggests that the precipitates were mixtures of different Zr species resulting from the decomposition of $[ZrL^1(H_{(2)}O)_x]^{n+}$ (**1**) at lower pH.

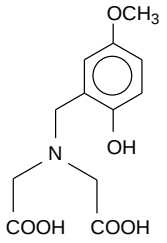

L^1

Chart 1

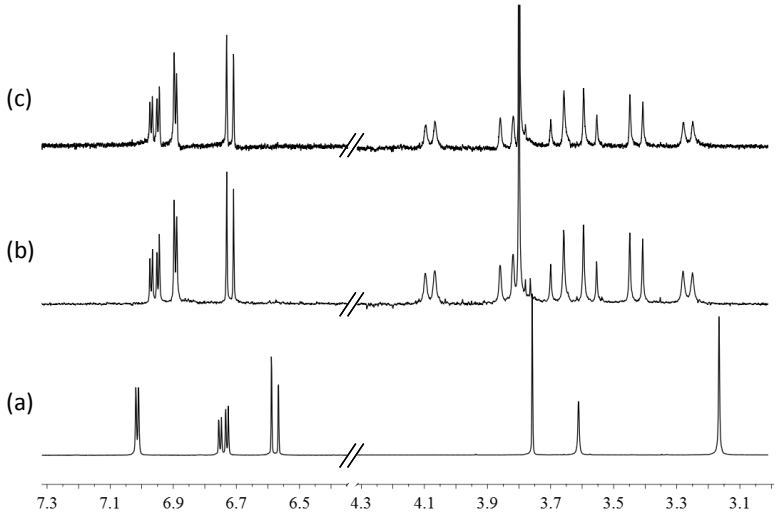

Fig. 1. 6.5 – 7 ppm and 3 – 4.3 ppm regions of the ^{1}H NMR spectra of (a) L^1 in D_2O at pD 12.2, (b) L^1 - $[Zr_4(OH)_8(H_2O)_{16}]Cl_8 \cdot 12H_2O$ mixtures at pD 6.9 and (c) L^1 - $[Zr_4(OH)_8(H_2O)_{16}]Cl_8 \cdot 12H_2O$ mixtures at pD 12.2; Zr : ligand ratio 1 : 1. Spectra were recorded immediately after mixing.

3.2. Hydrolysis of p-nitrophenyl phosphate

The ability of the zirconium complex **1** to promote phosphate monoester hydrolysis was studied using the activated model substrate NPP. Release of *p*-nitrophenolate was monitored in buffered solution at 25 °C by UV/Vis-spectroscopy. Orthophosphate was identified as the hydrolysis product by ^{31}P NMR spectroscopy (Fig. S1). Under pseudo-first order conditions, the hydrolysis reaction in neutral

solution is 10^4 times faster than the spontaneous hydrolysis of the phosphate monoester ($k = 8.2 \times 10^{-9}$ s^{-1}, pH 7, 25 °C [17,18]). The pH dependence of the pseudo-first order rate constant k_{obs} is displayed in Fig. 2. k_{obs} increases with decreasing pH. Unfortunately, it was not possible to determine rate constants for pH values below 6, as the catalyst precipitated out of the reaction mixture. Thus, the pH-rate profile does not allow any conclusions on the reaction mechanism. However, Lewis acid activation of the coordinated substrate and nucleophilic attack by a Zr-bound hydroxide is a likely scenario and in line with the usual mechanistic roles of metal-ions in phosphate ester hydrolysis. Zr-OH is known to form at pH < 1. Fig. 3 shows the dependence of k_{obs} on the concentration of **1** at pH 7.0 and 25 °C. Clean second-order kinetics are observed in the 0.25 – 2.0 mM concentration range with the second-order rate constant being 0.042 M^{-1} s^{-1}. In addition, the rate of **1**-mediated NPP hydrolysis was determined at different NPP concentrations. The linear relationship between the reciprocal initial rate ($1/v_o$) and the reciprocal concentration of the substrate indicates Michaelis-Menten behaviour. From the Lineweaver-Burk plot (Fig. 4) the hydrolysis rate of the bound substrate $k_{cat} = 2.7 \times 10^{-5}$ s^{-1} and the formation constant of the phosphate ester – zirconium complex $1/K_m = 806$ M^{-1} were determined.

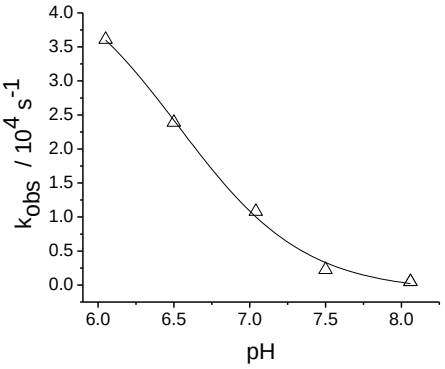

Figure 2. Rate-pH profile of the hydrolysis of NPP (5×10^{-5} M) in the presence of **1** (2 mM) in 50 mM buffer at 25 °C. *I* = 0.1 M (NaCl).

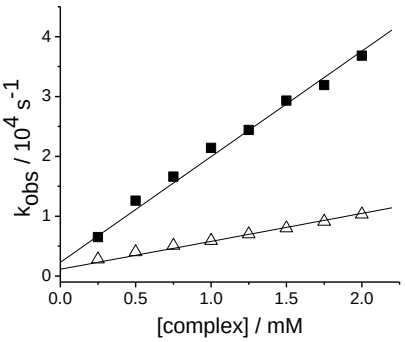

Figure 3. Dependence of the cleavage rate of NPP (5 x 10^{-5} M) on the concentration of **1** (△) and 2:1 mixtures of Zr^{4+} and L^2 (■) at 25 °C and pH 7.0; [buffer] = 50 mM (HEPES); *I* = 0.1 M (NaCl).

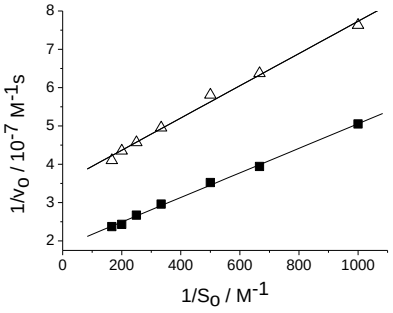

Figure 4. Lineweaver-Burk plots for the hydrolysis of NPP by **1** (1.0 mM) (△) and 2:1 mixtures of Zr^{4+} and L^2 (0.5 mM) (■); 25°C; pH 7; [buffer] = 50 mM (HEPES); *I* = 0.1 M (NaCl).

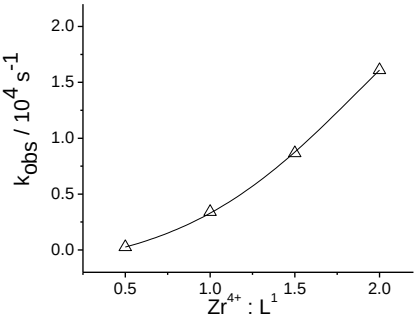

Figure 5. Dependence of the cleavage rate of NPP (5 x 10^{-5} M) on the metal to ligand ratio at pH 7.0 and 25 °C; [L^1] = 1 mM; pH = 7.0; [buffer] = 50 mM (HEPES); *I* = 0.1 M (NaCl).

NPP hydrolysis was also monitored using different ligand : Zr ratios. Interestingly, the ligand can keep up to 2 equivalents of Zr in solution. Fig. 5 shows a plot of the

pseudo-first order rate constant at pH 7 *vs.* Zr : ligand ratio. Evidently, k_{obs} increases exponentially, when an excess of Zr is added. The fact that no precipitation of Zr hydroxo species from neutral solution is observed, when L^1 and Zr^{4+} are mixed in a 1:2 ratio suggests that the ligand stabilizes polynuclear Zr species at pH 7 that are better catalysts than the mononuclear complex. Therefore we studied the formation and reactivity of Zr complexes of the dinucleating ligands L^2 and L^3 (Chart 2). The use of L^3 in a screening study on Zr complexes as catalysts for ATP hydrolysis has been previously reported by Jagoda and Krämer [9]. However, in their work an excess of ligand was used which makes the presence of dinuclear species in solution unlikely.

3.3. Dinuclear zirconium complexes

Addition of $[Zr_4(OH)_8(H_2O)_{16}]Cl_8 \cdot 12H_2O$ to solutions of L^2 and L^3 in D_2O in the pD range 5 – 10 resulted in a significant broadening of the ^1H NMR resonances (data not shown). The regions between 3 and 4 ppm where the methylene resonances are expected were particularly poorly resolved. Que *et al*. reported a dinuclear Ce^{4+} complex of L^3 with the two metal ions coordinating through the two deprotonated ligand side-arms and the bridging phenolate oxygen [13]. A similar complex can be expected to form with Zr^{4+}. ESI MS spectra were recorded in order to identify the species present in solution (Fig. S2). The ESI spectrum of a solution containing equimolar amounts of L^3 and Zr^{4+} shows a signal due to the isotopomers of $[ZrL^3]^-$ centred at m/z = 485.0 (100 %) as well as signals centred at m/z = 927.1, 949.1, 971.1, and 993.0 that can be assigned to $[Zr(L^3)_2+2Na^+ +3H^+]^-$, $[Zr(L^3)_2+3Na^+ +2H^+]^-$, $[Zr(L^3)_2+4Na^+ +H^+]^-$, and $[Zr(L^3)_2+5Na^+]^-$. Upon addition of a second equivalent of Zr^{4+} the dinuclear species $[Zr_2L^3(OH)_3Cl]^-$ and $[Zr_2L^3(OH)_2Cl_2]^-$ could be identified (isotopomer signals centred at m/z = 662.9 and 680.9, respectively) besides the mononuclear complexes $[ZrL_3]^-$ and $[Zr(L^3)_2+5Na^+]^-$ and inorganic Zr chloro complexes. Attempts to grow single crystals from solution were unsuccessful.

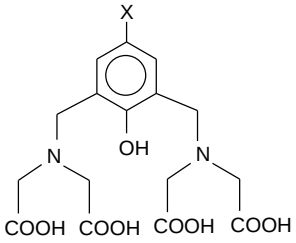

L^2: X = OCH_3
L^3: X = CH_3

Chart 2.

For the kinetic measurements solutions containing the dinuclear Zr complexes $[Zr_2L^2(H_{(2)}O)_xCl_y]^{n+}$ (**2**) and $[Zr_2L^3(H_{(2)}O)_xCl_y]^{n+}$ (**3**) were generated *in situ* by mixing the ligands with 0.5 equivalents of $[Zr_4(OH)_8(H_2O)_{16}]Cl_8 \cdot 12H_2O$. The rate-pH profiles, plots of k_{obs} *vs.* concentration and Lineweaver-Burk plots are shown in Figures 3, 4, 6 and S3 – S5. Again, ^{31}P NMR spectroscopy confirmed the formation of orthophosphate (Fig. S6). Kinetic data are summarised in Table 1. The second-order rate constants (0.17 M^{-1} s^{-1} for **2** and 0.18 M^{-1} s^{-1} for **3**; pH 7.0, 25 °C) are approximately four times larger than that of the mononuclear complex. It is worthy of note that **2** and **3** exhibit almost identical catalytic activity. This is in contrast to our recent study on mononuclear Ga complexes where an electron-donating methoxy substituent in *para* position to a coordinating phenolate oxygen led to an increase in the rate acceleration of phosphate diester hydrolysis [19].

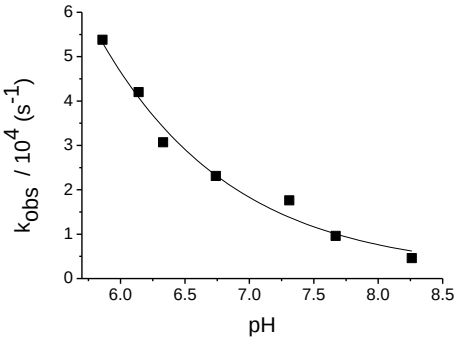

Figure 6. Rate-pH profile of the hydrolysis of NPP (5 x 10^{-5} M) by 2:1 mixtures of Zr^{4+} (2 mM) and L^2 (1 mM) in 50 mM buffer (HEPES) at 25 °C. *I* = 0.1 M (NaCl).

Since the 2:1 mixtures are only about 4 times more reactive than solutions of the mononuclear complex, it is not clear, if the difference in reactivity is due to the presence of dinuclear species that have a higher overall charge than the mononuclear complex **1** (3+ *vs.* 1+ not taking possible hydroxo ligands into account) or if there is some co-operativity between the two metal ions in the dinuclear complex. As in the case of the mononucleating ligand L^1, aqueous solutions remained homogeneous, when an excess of Zr^{4+} was applied. Up to four equivalents of Zr can be added at pH 7 before precipitation is observed. Fig. S7 shows the increase of the rate constant with increasing Zr : ligand ratio for L^3.

To investigate whether neutral solutions of the Zr complexes with the dinucleating ligands also hydrolyze phosphate monoesters with poorer leaving groups than *p*-nitrophenolate, L^3 was mixed with 0.5 equivalents $[Zr_4(OH)_8(H_2O)_{16}]Cl_8 \cdot 12H_2O$ and reacted with one equivalent of phenyl phosphate (PP) in D_2O at pD 7.0. The appearance of a peak at 2.16 ppm in the ^{31}P NMR spectrum indicated the formation of orthophosphate (Fig. S8). Integration of the ^1H NMR spectra showed that approximately 50 % of the substrate have been hydrolyzed after 4 d at 40 °C. When the rate constant for the uncatalyzed reaction [20] is extrapolated to 40 °C and pH 7, the rate acceleration provided by one equivalent of the dinuclear complex can be estimated to be in the order of 10^5 to 10^6-fold. Although signal overlap prevented a detailed kinetic analysis, the present data suggest that **3** is more reactive towards PP than towards the more activated substrate NPP. This is a notable feature, as metal complexes that are efficient catalysts for the hydrolysis of phosphate esters with good leaving groups are not necessarily equally reactive towards less activated substrates. Indeed, many metal catalysts that provide large rate accelerations for hydrolyzing *p*-nitrophenyl phosphate esters fail to hydrolyze or show significantly lower reactivity towards substrates with poor leaving groups [21-23].

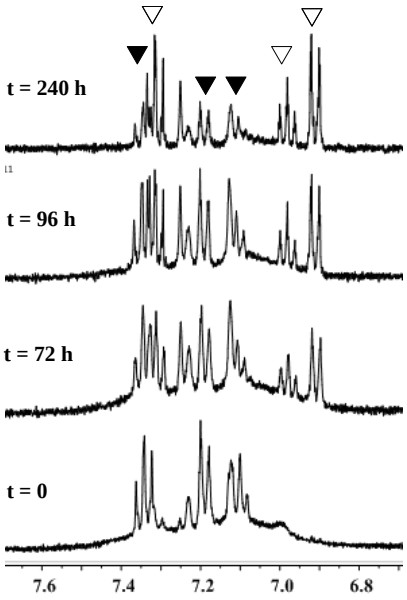

Figure 7. Aromatic region of the ^{1}H NMR spectra of phenyl phosphate (10 mM) in the presence of L^3 (10 mM) and Zr^{4+} (20 mM) at pD 7.0 and 40 °C. ▼ = phenyl phosphate; ∇ = hydrolysis product

3.4. Hydrolysis of bis(p-nitrophenyl) phosphate

To compare the reactivity of the Zr complexes towards phosphate mono- and diesters, the effects of solutions containing the dinuclear Zr complexes **2** and **3** on the cleavage rate of bis(*p*-nitrophenyl) phosphate (BNPP) were investigated. However, in all cases the absorbance *vs.* time traces showed an induction period the length of which varied non-systematically with pH. It is unlikely that these lag times are due to slow substrate binding, as fast ligand exchange kinetics are characteristic for the Zr^{4+} ion. In the case of heterodinuclear Fe(III)M(II) complexes reported in the literature [24], similar lag times in the onset of phosphate diester hydrolysis have been attributed to the slow transformation of the metal complexes into the respective active species. It should be noted that letting the buffered metal complex solutions stand at room temperature for 30 min. before adding the substrate had no effect on the induction periods. Although the induction periods hampered the accurate determination of rate constants, initial rates were estimated from the linear segments of the absorbance - time traces after the lag time. Between pH 5.5 and 8.5 (25 °C) approximate values for k_{obs} were in the range 0.1 x 10^{-5} - 2 x 10^{-5} s^{-1} for **2** and **3** corresponding to 10^5 – 10^6-fold rate accelerations over the uncatalyzed reaction [25].

Interestingly, the hydrolysis of the phosphate monoester NPP in solutions of **2** and **3** proceeds faster than does the cleavage of the phosphate diester BNPP. Under the same experimental conditions (pH 7, 25 °C), the pseudo-first order rate constant for mono ester hydrolysis mediated by a solution of **3** (2.1 x 10^{-4} s^{-1}) is almost 2 orders of magnitude higher than that for phosphate diester hydrolysis (3.6 x 10^{-6} s^{-1}). By contrast, the $ZrCl_4$-mediated hydrolyses of BNPP and NPP in weakly acidic solution proceed with similar rates (k_{obs} = 6 x 10^{-3} s^{-1} for the hydrolysis of BNPP by 5 mM $ZrCl_4$, pH 4, 20 °C and 3.4 x 10^{-3} s^{-1} for NPP hydrolysis [6]). There are very few examples for metal complexes that selectively hydrolyze phosphate monoesters over phosphate diesters. Komiyama *et al*. found that Ce^{IV} ions in concentrated buffer solution hydrolyze the monophosphate of 2'-deoxyadenosine (dAp) 580-fold faster than the dinucleotide d(ApA) [26]. It has been pointed out that such selectivity can be exploited for the removal of a terminal phosphate group in various biotechnological applications [26].

3.5. Activation parameters

The temperature influence on the hydrolysis reaction was investigated and the activation parameters for the reaction mediated by the zirconium complexes of L^1 – L^3 were determined by fitting the kinetic data to the Eyring and Arrhenius equations,

$$\ln\left(\frac{k_{obs}}{T}\right) = -\frac{\Delta H^{\ddagger}}{RT} + \ln\left(\frac{k}{h}\right) + \frac{\Delta S^{\ddagger}}{R} \quad \text{and} \quad \ln k_{obs} = \ln A - \frac{E_a}{RT};$$

k = Boltzmann constant, h = Planck constant, R = molar gas constant.

Eyring and Arrhenius plots are displayed in Figs. 8, S9 and S10, values of $\Delta S^{\ddagger}$, $\Delta H^{\ddagger}$, and E_a are listed in Table 2. From the data, it can be concluded that in all three cases NPP hydrolysis takes place through a similar mechanism. The negative values for the activation entropy are consistent with an associative substitution mechanism as observed for the metalloenzyme-catalyzed phosphate monoester hydrolysis [27]. A shift from the dissociative mechanism of the uncatalyzed reaction to an associative transition state with more nucleophilic participation upon metal ion coordination to the phosphate ester seems to be a general feature of metal-mediated phosphate monoester hydrolysis [23,28,29].

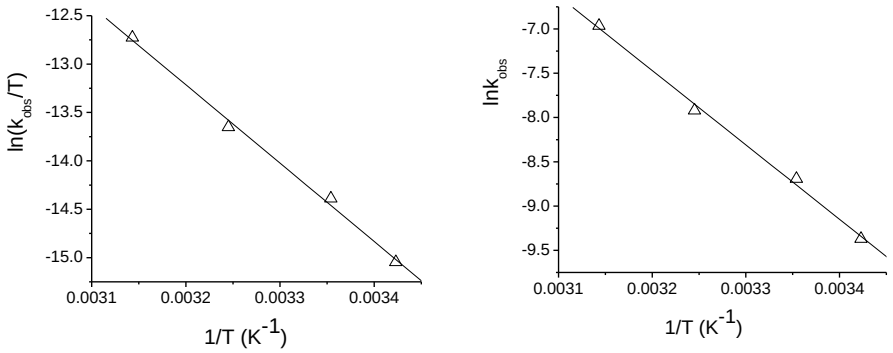

Figure 8. Eyring (left) and Arrhenius (right) plots for the hydrolysis of NPP (5 x 10^{-5} M) by **1** (2 mM) at 25°C and pH 7; [buffer] = 50 mM (HEPES); *I* = 0.1 M (NaCl).

4. Conclusions

The ligands L^1, L^2 and L^3 form water-soluble Zr complexes in the pH range 6 to 12 and enable phosphate monoester hydrolysis by homogeneous Zr^{IV} solutions at neutral pH. Although a detailed kinetic analysis of the cleavage of phenyl phosphate was hampered by significant signal overlap in the ^{1}H NMR spectra, solutions of the Zr complexes of the dinucleating ligands seem to be more reactive towards phosphate monoesters with poorer leaving groups than towards phosphate monoesters with better leaving groups. While a 2:1 mixture of Zr^{4+} and L^3 provides a *ca.* 10^4 fold rate acceleration of NPP hydrolysis under pseudo-first order conditions at pH 7, one equivalent reduces the half-life for the hydrolysis of phenyl phosphate to *ca.* 4 days corresponding to a remarkable $10^5 – 10^6$ rate acceleration.

Acknowledgements

Financial support from Science Foundation Ireland (Stokes Lectureship to A.E.) is gratefully acknowledged. F. C. thanks NUI Galway for a College of Science Fellowship.

Supplementary Material

^{31}P NMR spectra, ESI-MS data, rate-pH profile, concentration dependence and Lineweaver-Burk plot for **3**-mediated NPP hydrolysis; plot of k_{obs} *vs.* Zr:L^3 ratio, Eyring and Arrhenius plots for the hydrolysis of NPP in the presence of zirconium complexes of L^2 and L^3.

References

[1] C. Lad, N.H. Williams, R. Wolfenden, Proc. Natl. Acad. Sci., USA 100 (2003) 5607 – 5610.

[2] L.R. Gahan, S.J. Smith, A. Neves, G. Schenk, Eur. J. Inorg. Chem. (2009) 2745 – 2758 and refs therein.

[3] J. Chin, Acc. Chem. Res. 24 (1991) 145 – 152.

[4] J.P. Guthrie, J. Am. Chem. Soc. 99 (1977) 3991 – 4001.

[5] E. Bamann, Angew. Chem. 52 (1939) 186 – 188.

[6] R. Ott, R. Krämer, Angew. Chem. Int. Ed. 37 (1998) 1957 – 1960.

[7] R.A. Moss, J. Zhang, K.G. Ragunathan, Tetrahedron Lett. 39 (1998) 1529 – 1532.

[8] J.F. Kennedy, S.A. Barker, J.D. Humphreys, *J. Chem. Soc., Perkin Trans. 1* (1977) 753 – 757.

[9] M. Jagoda, R. Krämer, Inorg. Chem. Commun. 8 (2005**)** 697 – 699.

[10] E. Stulz, C. Leumann, Chem. Commun. (1999) 239 – 240.

[11] E. Stulz, H.-B. Bürgi, C. Leumann, Chem. Eur. J. 6 (2000**)** 523 – 536.

[12] A. Du Moulinet d'Hardemare, O. Jarjayes, F. Mortini, Synth. Commun. 34 (2004**)** 3975 – 3988.

[13] M.E. Branum, A.K. Tipton, S. Zhu, L. Que, J. Am. Chem. Soc. 123 (2001) 1898 – 1904.

[14] P.K. Glasoe, F.A. Long, J. Phys. Chem. 64 (1960) 188 – 190.

[15] K. Mikkelsen, S.O. Nielsen, J. Phys. Chem. 64 (1960**)** 632 – 637.

[16] S. Espinosa, E. Bosch, M. Roses, J. Chromatogr. A 964 (2002) 55 – 66.

[17] A.J. Kirby, W.P. Jencks, J. Am. Chem. Soc. 87 (1965) 3209 – 3216.

[18] D.H. Vance, A.W. Czarnik, J. Am. Chem. Soc. 115 (1993) 12165 – 12166.

[19] F. Coleman, M.J. Hynes, A. Erxleben, Inorg. Chem. 49 (2010**)** 6725 – 6733.

[20] The rate constant for the spontaneous hydrolysis of the phenyl phosphate dianion at 39 °C is 10^{-12} s^{-1} (ref [1]).

[21] J.S. Seo, R.C. Hynes, D. Williams, J. Chin, J. Am. Chem. Soc. 120 (1998) 9943 – 9944.

[22] N.H. Williams, W. Cheung, J. Chin, J. Am. Chem. Soc. 120 (1998) 8079 – 8087.

[23] N.H. Williams, A.-M. Lebuis, J. Chin, J. Am. Chem. Soc. 121 (1999) 3341 – 3348.

[24] M. Jarenmark, M. Haukka, S. Demeshko, F. Tuczek, L. Zuppiroli, F. Meyer, E. Nordlander, Inorg. Chem. 50 (2011) 3866 – 3887.

[25] J. Chin, M. Banaszczyk, V. Jubian, X. Zou, J. Am. Chem. Soc. 111 (1989) 186 – 190.

[26] S. Miyama, H. Asanuma, M. Komiyama, J. Chem. Soc., Perkin Trans. 2 (1997) 1685 – 1688.

[27] K. Ichikawa, M. Tarnai, M.K. Uddin, K. Nakata, S. Sato, J. Inorg. Biochem. 91 (2002) 437 – 450.

[28] R. Breslow, I. Katz, J. Am. Chem. Soc. 90 (1968) 7376 – 7377.

[29] I.E. Catrina, A.C. Hengge, J. Am. Chem. Soc. 121 (1999) 2156 – 2163.

Table 1. Kinetic data for the hydrolysis of NPP at pH 7.0 and 25 °C

Ligand	Zr:ligand ratio	k (M^{-1} s^{-1})	v_{max} (10^8 M s^{-1})	k_{cat} (10^4 s^{-1})	$1/K_m$ (M^{-1})
L[1]	1:1	0.042	2.72	0.27	806
L[2]	2:1	0.17	5.47	1.1	556
L[3]	2:1	0.18	5.51	1.1	565

Table 2. Activation parameters for the hydrolysis of NPP at pH 7.0

Ligand	Zr:ligand ratio	$\Delta S^{\ddagger}$ (J K^{-1})		$\Delta H^{\ddagger}$ (kJ mol^{-1})	E_a (kJ mol^{-1})
L[1]	1:1	-92.0	67.3	69.9	
L[2]	2:1	-75.6	71.4	73.9	
L[3]	2:1	-98.6	64.1	66.6	